



Uniformly doped bioactive strontium ions chelate extracellular matrix scaffolds for bone repair

Yuke Li^{a,1}, Yi Zhang^{b,1}, Yuhua Liu^{a,*}, Mei Wang^c, Lin Tang^a

^a Department of Prosthodontics, Peking University School and Hospital of Stomatology, National Center for Stomatology, National Clinical Research Center for Oral Diseases, National Engineering Research Center of Oral Biomaterials and Digital Medical Devices, Beijing 100081, China

^b Department of General Dentistry II, Peking University School and Hospital of Stomatology, National Center for Stomatology, National Clinical Research Center for Oral Diseases, National Engineering Research Center of Oral Biomaterials and Digital Medical Devices, Beijing 100081, China

^c Department of Stomatology, Beijing Chao-Yang Hospital, Capital Medical University, Beijing 100020, China

ARTICLE INFO

Keywords:

Strontium
Small intestinal submucosa
Coordination
Porous materials
Biomaterials

ABSTRACT

This paper describes a novel natural extracellular matrix-derived scaffold composite prepared through a coordination reaction between small intestinal submucosa (SIS) and strontium (Sr) ions. The physicochemical and biological properties of the Sr/SIS composite scaffold were investigated. The Sr/SIS complex had a porous structure and a uniform distribution of Sr²⁺. The coordination bond of Sr-SIS provides the Sr/SIS scaffolds with improved mechanical properties and sustained Sr²⁺ release. Controlled release of Sr²⁺ enhanced cell proliferation and osteogenic differentiation. The 1.5 wt% Sr/SIS scaffold had the best osteogenesis effect among the experimental groups, indicating its potential as a biomaterial for bone tissue engineering.

1. Introduction

Bone tissue engineering is a promising strategy for the treatment of bone defects. Biomaterial-based functional scaffolds have been extensively researched. Small intestinal submucosa (SIS) is a natural extracellular matrix-derived material with a mimetic three-dimensional microenvironment primarily composed of type I & III collagens, as well as glycosaminoglycans, adhesion molecules, and cytokines [1]. SIS is suitable for bone tissue engineering. Current research on SIS scaffold has focused on functionalization with therapeutic agents to achieve favorable cellular responses and aid bone regeneration [2].

Strontium (Sr) dose-dependently promotes or inhibits osteoblast functions. Its advantages include no risk of decomposition, low sensitivity to microenvironmental conditions, and low cost [3]. The construction of a localized delivery system that combines Sr²⁺ with a scaffold is thus a favorable strategy. However, sudden ion release can be toxic to cells and cause unwanted side effects [4]. Sr-containing composite scaffolds that exhibit long-lasting and controlled ion release are highly desirable. Recently, various controlled Sr²⁺ release scaffolds have been constructed by substituting Sr²⁺ for hydroxyapatite and bio-glass [5,6], adding graphene oxide [7], and self-assembly/mineralization of collagen [8], etc.

The collagen which is abundant in SIS can interact with a wide range of metal ions. The chelation of collagen and its derivatives with metal ions has been extensively studied [9]. But the construction of a Sr/SIS complex system for bone tissue regeneration has not been reported. Hence, we reported the novel Sr/SIS complexes with controlled Sr²⁺ release. The incorporated Sr²⁺ enhanced the osteogenic activity and mechanical properties of SIS scaffolds, providing a simple, effective, and affordable bone tissue engineering option.

2. Experimental

2.1. Scaffold preparation

The SIS scaffold was fabricated as described previously [10]. Briefly, SIS solution (1%, w/v) was produced by dissolving decellularized SIS powder in deionized water with acetic acid (3%, v/v) and pepsin (0.1%, w/v). After pouring into molds, the solution was precooled at -20 °C and -80 °C for 24 h and lyophilized at -80 °C in a freeze dryer (Freezone; Labconco, USA). SIS scaffolds served the control group. To prepare the Sr/SIS scaffold, SIS solution was prepared as described above. SrCl₂ aqueous solutions of varying concentrations were mixed with an equal volume of SIS solution to obtain mixed solutions containing 1%, 1.5%,

* Corresponding author.

E-mail address: liuyuhua@bjmu.edu.cn (Y. Liu).

¹ The authors contributed equally to this article.

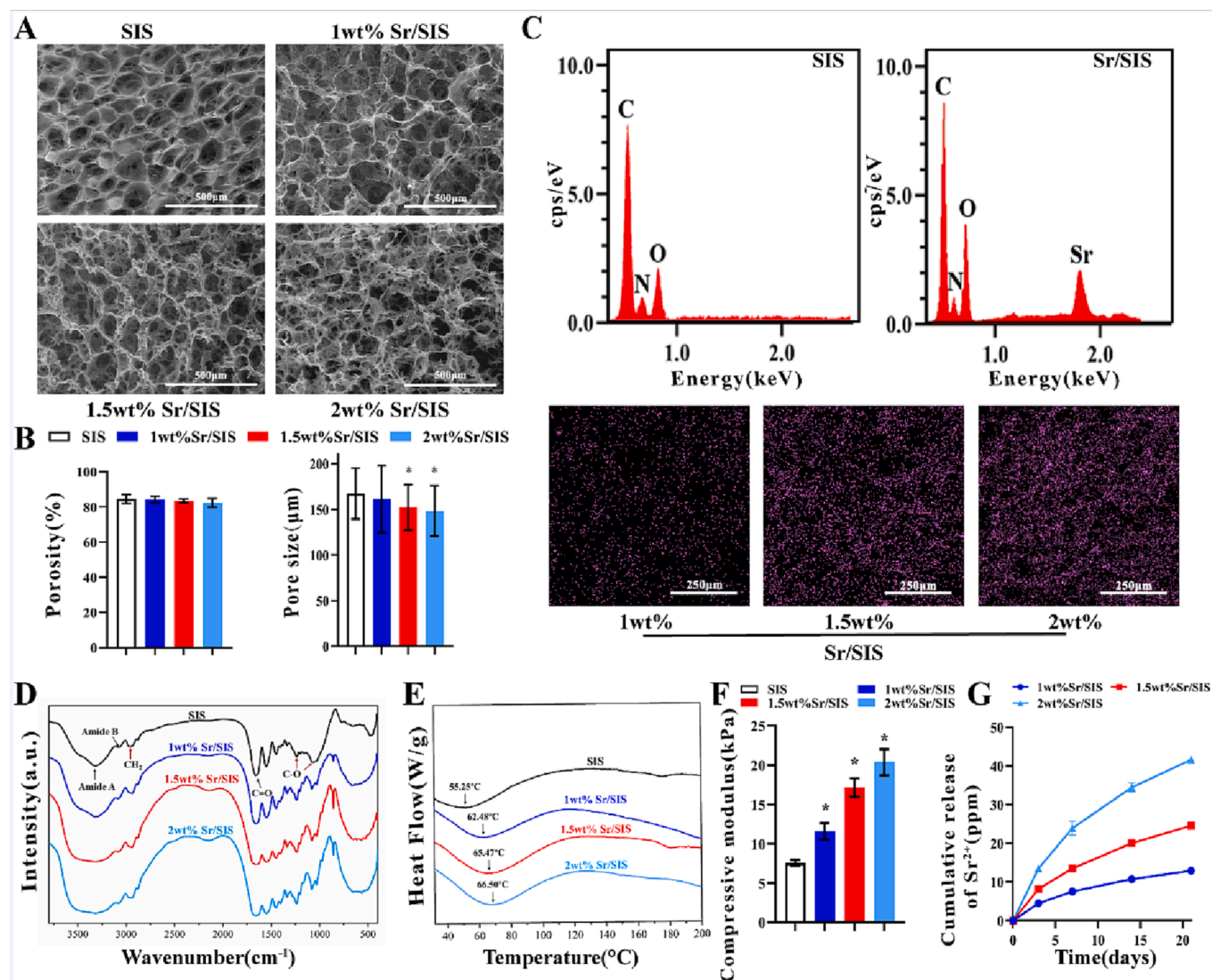


Fig. 1. A) ESEM images of the SIS and Sr/SIS scaffolds (300X); B) Porosity and pore size; C) EDS and Mapping analysis; D) FTIR analysis; E) DSC profiles; F) Compressive strength; G) Cumulative Sr^{2+} release. * $P < 0.05$.

or 2% (w/v) SrCl_2 . The pH values of the mixed solutions were adjusted to 7, and the solutions were stored at 37 °C for 2 h to facilitate reaction. Then the solutions were poured into molds and lyophilized as mentioned above. Samples were crosslinked by 1-ethyl-3-(3-dimethylaminopropyl) carbodiimide/N-hydroxysuccinimide (50 mM/25 mM) in 95% ethanol for 24 h. The abbreviations of scaffolds were shown in S1.

2.2. Characterization

The morphologies of the lyophilized scaffolds were characterized by environmental scanning electron microscopy (ESEM; Quanta 200F; FEI, USA), pore sizes by ImageJ software (National Institutes of Health, USA), and porosity by the liquid displacement method. Fourier transform-infrared (FTIR) and energy-dispersive spectroscopy (EDS) analyzed chemical compositions. Samples from each group ($n=3$) were analyzed by differential scanning calorimetry (DSC3; Mettler Toledo, Switzerland) at a scan rate of 5°C/min from 30°C to 200°C. The compressive strength of each group ($n=3$) was measured using a universal testing machine (model 336; Instron, USA) at 1 mm/min. Sr^{2+} release properties of the Sr/SIS scaffolds ($n=3$ /group) were measured by inductively coupled plasma-atomic emission spectrometry in phosphate-buffered saline at 37 °C (Model 5110; Agilent, USA).

2.3. Cell proliferation and viability

Human bone marrow stem cells (hBMSCs) were seeded onto the scaffolds at a density of 1.5×10^4 cells ($n=3$ /group). Cell counting kits were used to measure hBMSCs' proliferation on scaffolds after 1, 3, 5, 7, and 9 days of incubation (CCK-8; Dojindo, Japan). 2×10^4 hBMSCs were incubated on each scaffold for 1 day ($n=3$ /group). A live/dead viability assay (KeyGen, China) was used to identify the live and dead cells, which were visualized by confocal laser scanning microscopy (TCS SP8 X; Leica, Germany).

2.4. In vitro osteogenic ability

3×10^4 hBMSCs were seeded on each sample ($n=3$ /group). Alkaline phosphatase (ALP) staining was conducted using a nitroblue tetrazolium/5-bromo-4-chloro-3-indolyl phosphate staining kit (Beyotime Biotechnology, China) after 7 and 14 days of osteo stimulation. ALP activity was also assessed using an ALP activity assay kit (Jiancheng Technology, China). Calcium nodules on the scaffolds were stained with 1 wt% alizarin red dye after 21 days in osteogenic medium and were quantified by immersing in 100 mM cetylpyridinium chloride monohydrate aqueous solution (Sigma, USA).

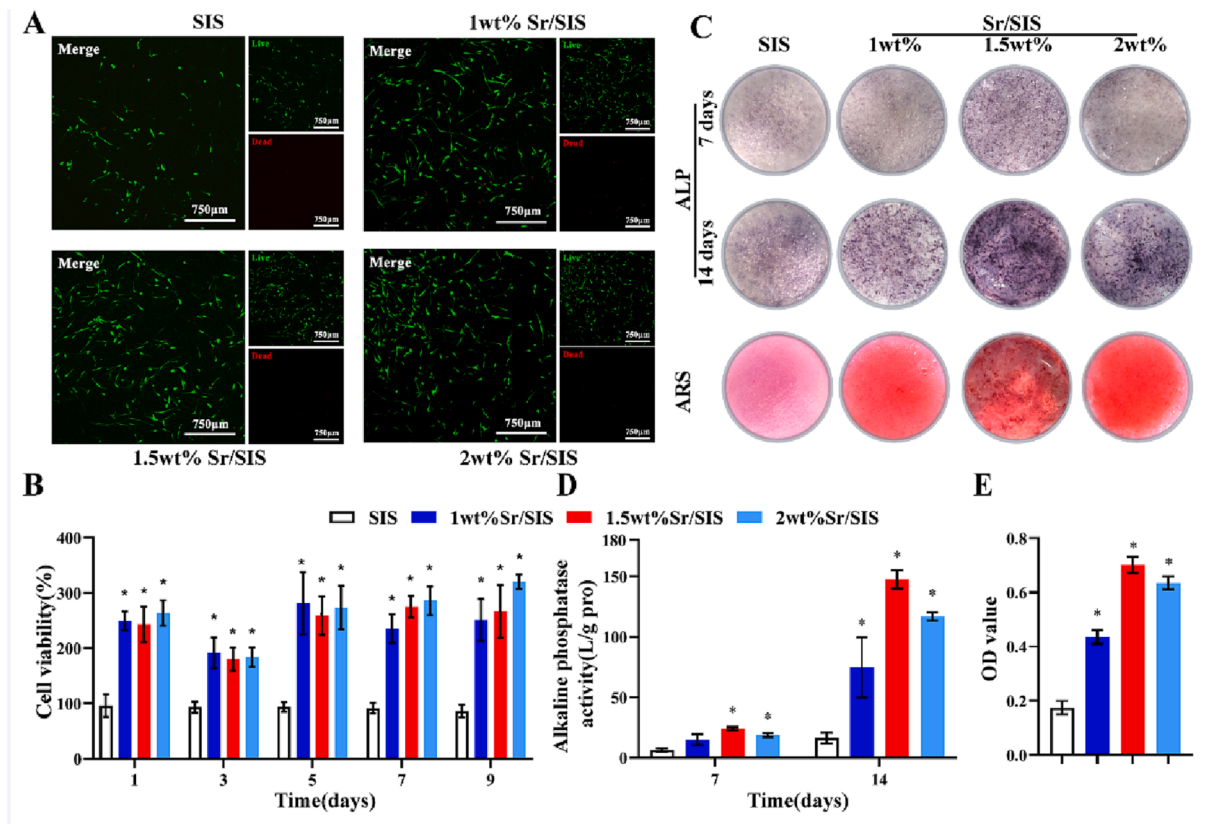


Fig. 2. A) Live/dead viability assay; B) CCK-8 assay; C) ALP and alizarin red staining; D) Quantitative results of ALP activity; E) Semi-quantitative results of mineralized nodules. * $P < 0.05$.

2.5. Statistical analysis

All experiments were performed in triplicate. One-way analysis of variance followed by Tukey's post hoc test was performed using SPSS 22.0 software (IBM, USA) and $P < 0.05$ was considered statistically significant.

3. Results and discussion

Fig. 1A presented ESEM images of the surface morphology of the SIS and Sr/SIS scaffolds. These materials had highly porous structures with closely connected pores that facilitated angiogenesis and osteogenesis [11]. It was speculated that the added Sr^{2+} coordinated with collagen fibers and affected the volume of ice crystals formed in the mixed solution during precooling [12], the Sr/SIS scaffold seemed to form more microporous structures as strontium was added (Fig. 1B). But these data were preliminary and it was so far only speculation. The results of EDS were presented in Fig. 1C. The characteristic peak of Sr was detected in the Sr/SIS scaffolds, no other elemental impurities were detected. Mapping analysis (Fig. 1C) showed that Sr was uniformly distributed and that became more evident as Sr content increased. The FTIR spectra presented in Fig. 1D showed that the absorption peaks of SIS at 1,236 and 1,063 cm^{-1} shifted upon addition of Sr^{2+} , consistent with the formation of chelates between SIS carboxyl groups and Sr^{2+} [13]. The shift to lower frequency of the $-\text{CH}_2$ group stretching vibration peak observed at 2,966 cm^{-1} also suggested that Sr^{2+} exerted an electron withdrawal effect on chelate formation. DSC provided a wealth of information concerning the thermal degeneration of collagen. The specific binding of metal ions to high-energy sites of collagen-like substances reduced internal energy and increased secondary structure stability through crosslinking, resulting in a high denaturation temperature [9]. Fig. 1E showed that Sr/SIS scaffolds had higher denaturation temperatures than

SIS scaffold, consistent with the chelation reaction thus the thermodynamic stability of the Sr/SIS scaffolds was improved. The compressive strength of the scaffolds was also measured (Fig. 1F). The Sr/SIS scaffolds had higher compressive strength than the SIS scaffold. This result was similar to that of Liu et al, suggesting that Sr^{2+} may act as a "crosslinker", improving the mechanical strength of scaffolds [14]. The scaffolds exhibited a sudden Sr^{2+} release in the early stage (Fig. 1G), presumably due to the dissolution of unchelated Sr^{2+} on the surface of the scaffolds. The release rate of Sr^{2+} then gradually decreased but still incurred after 21 days, indicating that the remaining Sr^{2+} was bound to the SIS. According to characterizations above, the chelated Sr^{2+} could be released sustainably. The Sr/SIS scaffolds with appropriate pore sizes and porosity had better mechanical properties for bone tissue engineering than SIS scaffolds which warranted further research in bone regeneration.

Biocompatibility of scaffolds is a prerequisite for bone regeneration. Fig. 2A&B showed that all groups had few dead cells and the Sr/SIS scaffolds promoted cell proliferation more effectively than the SIS scaffolds. All scaffolds were found to be biocompatible, and their interconnected structures might have facilitated the survival and growth of hBMSCs [11]. Moreover, the presence of Sr^{2+} enhanced the proliferation of hBMSCs as reported previously [3].

Furthermore, the effect of the scaffolds on bone repair was also studied. ALP activity and calcified nodules were used as markers of early and late osteogenic differentiation of hBMSCs, respectively. ALP and alizarin red staining (Fig. 2C) showed that Sr/SIS groups had more stained areas than SIS groups. Quantitative analysis showed a similar trend (Fig. 2D&E), the expression of ALP and formation of mineralized nodules were significantly enhanced in the Sr/SIS groups compared with the SIS group ($P < 0.05$), which suggested that Sr/SIS composites could promote bone repair. This is consistent with previous findings that Sr^{2+} enhanced hBMSC osteogenic differentiation [15]. Notably, previous

research indicated that the osteogenic effect of Sr had an optimal concentration interval rather than a first-order dependence [16]. The 1.5 wt % Sr/SIS scaffolds had the highest ALP activity and calcium deposition among all groups, indicating an appropriate Sr level in Sr/SIS. Overall, the Sr/SIS scaffolds achieved better physiochemical, biocompatible, and bioactive properties for bone substitutes in vivo.

4. Conclusion

This study developed a novel Sr/SIS composite with a porous and interconnected three-dimensional structure. Incorporation of Sr improved the mechanical properties of the scaffold and ensured sustained local delivery of bioactive Sr²⁺. The Sr/SIS scaffold exhibited good cytocompatibility and promoted osteogenic differentiation of hBMSCs. Although these results indicate that Sr/SIS scaffolds can be used in bone tissue regeneration, additional in-depth studies are needed to define the mechanism of action.

CRedit authorship contribution statement

Yuke Li: Methodology, Validation, Writing – original draft, Data curation, Resources. **Yi Zhang:** Investigation, Formal analysis, Writing – original draft, Data curation. **Yuhua Liu:** Conceptualization, Writing – review & editing, Supervision. **Mei Wang:** Investigation, Formal analysis. **Lin Tang:** Writing – review & editing, Supervision.

Declaration of Competing Interest

The authors declare that they have no known competing financial interests or personal relationships that could have appeared to influence

the work reported in this paper.

Data availability

Data will be made available on request.

Appendix A. Supplementary data

Supplementary data to this article can be found online at <https://doi.org/10.1016/j.matlet.2023.134083>.

References

- [1] S.F. Badylak, D.O. Freytes, T.W. Gilbert, *Acta Biomater.* 5 (2009) 1–13.
- [2] M.A. Fernandez-Yague, S.A. Abbah, L. McNamara, et al., *Adv. Drug Deliv. Rev.* 84 (2015) 1–29.
- [3] E. O'Neill, G. Awale, L. Daneshmandi, et al., *Drug Discov. Today.* 23 (2018) 879–890.
- [4] Y.F. Zheng, X.N. Gu, F. Witte, *Mater. Sci. Eng. R-Rep.* 77 (2014) 1–34.
- [5] L. Gritsch, M. Maqbool, V. Mourino, et al., *J. Mater. Chem. B.* 7 (2019) 6109–6124.
- [6] H. Manoochehri, M. Ghorbani, M. Moosazadeh Moghaddam, et al., *Sci. Rep.* 12 (2022) 10160.
- [7] Y. Chen, Z. Zheng, R. Zhou, et al., *ACS Appl. Mater. Interfaces.* 11 (2019) 15986–15997.
- [8] H. Liu, M. Lin, X. Liu, et al., *Bioact. Mater.* 5 (2020) 844–858.
- [9] C. Zhu, Y. Sun, Y. Wang, et al., *Mater. Sci. Eng. C Mater. Biol. Appl.* 33 (2013) 2611–2619.
- [10] B. Li, M. Wang, Y. Liu, et al., *Colloid Surf. B-Biointerfaces.* 212 (2022), 112370.
- [11] Y. Li, Y. Xiao, C. Liu, *Chem. Rev.* 117 (2017) 4376–4421.
- [12] J. Grenier, H. Duval, F. Barou, *Acta Biomater.* 94 (2019) 195–203.
- [13] D.W. Urry, *Proc. Natl. Acad. Sci. USA.* 68 (1971) 810–814.
- [14] J. Liu, H. Zeng, P. Xiao, et al., *ACS Omega.* 5 (2020) 24477–24486.
- [15] F. Yang, D. Yang, J. Tu, et al., *Stem Cells.* 29 (2011) 981–991.
- [16] M. Pilmane, K. Salma-Ancane, D. Loca, et al., *Mater. Sci. Eng. C Mater. Biol. Appl.* 78 (2017) 1222–1230.